Small-on-Large Fractional Derivative–Based Single-Cell Model Incorporating Cytoskeleton Prestretch

M. Fraldi[1]; A. Cugno[2]; A. R. Carotenuto, Ph.D.[3]; A. Cutolo, Ph.D.[4]; N. M. Pugno[5]; and L. Deseri[6]

Abstract: In recent years, experimental evidences have suggested important direct implications of viscoelasticity of human cells and cell cytoskeleton dynamics on some relevant collective and single-cell behaviors such as migration, adhesion, and morphogenesis. Consequently, the mechanical properties of single cells and how cells respond to mechanical stimuli have been at the center of a vivid debate in the scientific community. By referencing important experimental findings from the literature that have shown that human metastatic tumor cells are approximately 70% softer than benign cells, independently from the cell lines examined, the present authors have very recently theoretically demonstrated that these differences in stiffness might be exploited to mechanically discriminate healthy and cancer cells, for example, through low-intensity therapeutic ultrasound. In particular, by using a generalized viscoelastic paradigm combining classical and fractional derivative–based models, it has been found that selected frequencies (from tens to hundreds of kilohertz) are associated with resonancelike phenomena that are prevailing on thermal fluctuations and hence could be, at least in principle, helpfully utilized for both targeting and selectively attacking tumor cells. With the aim of investigating the effect of the prestress (for instance, induced in protein filaments during cell adhesion) on the overall cell stiffness and, in turn, on its in-frequency response, a simple multiscale scheme is proposed in this paper to bottom-up enrich the spring-pot-based viscoelastic single-cell models by incorporating finite elasticity and thereby determining through sensitivity analyses the role played by the stretched state of the cytoskeletal elements on the cell vibration. **DOI: 10.1061/(ASCE)EM.1943-7889.0001178.**

Introduction

From the mechanical point of view, single human cells can be seen as viscoelastic systems (Del Piero and Deseri 1997; Deseri et al. 2006; Fraldi et al. 2015; Haase and Pelling 2015; Tschoegl 1989). However, unlike inorganic materials, living soft matter is inhomogeneous and generally hierarchically organized (Chen and Pugno 2013; Fraldi 2014; Fraldi and Cowin 2004; Huang et al. 2014; Pugno et al. 2012) and thus reacts, over different timescales, to mechanical stimuli by simultaneously involving protein filaments and supramolecular and molecular structures present at different scale levels. In fact, the cell hierarchical organization works as a complex transducer device that converts mechanical signals in biochemical and physical coordinated events, which govern the mechanobiology and the mechanosensing of the whole cell, regulating differentiation, growth, morphogenesis, and (through polymerization/depolymerization-based cytoskeleton structural rearrangements) migration and adhesion phenomena at the single-cell and macroscopic (tissue) levels (Delsanto et al. 2008; DuFort et al. 2011; Guiot et al. 2006; Paszek et al. 2014).

Three main mechanically relevant structural systems can be recognized in a human cell, a complex factory that makes proteins and tissue materials (Cowin and Doty 2007): the 10-nm-thick, very deformable (0.1–1 kPa) lipid bilayer (the cell membrane); the gel-like viscoelastic cytosol; and the cytoskeleton, the main bearing cell structure constituted by a network of elastic protein filaments that are embedded within the cytosol and anchored to both the nucleus and the cell membrane, which mediates mechanical signals, regulates cell shapes during migration and adhesion, and somehow protects the cell. Microtubules (tubes with diameters of approximately 25 nm made up of two subunits of spiraling tubulin), actin, and intermediate filaments (7- and 10-nm-diameter twisted double-woven and interwoven rope strands of actin) are the main cytoskeletal filaments, whose assembling/disassembling (polymerization/depolymerization) drives cell motility and spreading (Bao and Suresh 2003; Brunner et al. 2009).

A significant number of scientific works have been dedicated to the analysis of the response of human cells to mechanical stimuli in recent years and, because of the complexity of the systems, several behaviors still remain not completely understood. Recently, it has

[1]Professor, Dept. of Structures for Engineering and Architecture, Polytechnic School, College of Engineering, Univ. of Napoli Federico II, 80138 Napoli, Italy; Interdisciplinary Research Center for Biomaterials, Polytechnic School, College of Engineering, Univ. of Napoli Federico II, 80138 Napoli, Italy; Institute of Applied Sciences and Intelligent Systems, National Research Council of Italy, Italy (corresponding author). E-mail: fraldi@unina.it

[2]Ph.D. Student, Dept. of Structures for Engineering and Architecture, Polytechnic School, College of Engineering, Univ. of Napoli Federico II, 80138 Napoli, Italy; Dept. of Civil, Environmental and Mechanical Engineering, Univ. of Trento, 38122 Trento, Italy. E-mail: andrea.cugno@unitn.it

[3]Dept. of Chemical, Materials, and Production Engineering, Univ. of Naples Federico II, 80138 Napoli, Italy. E-mail: angelorosario.carotenuto@unina.it

[4]Dept. of Chemical, Materials, and Production Engineering, Univ. of Naples Federico II, 80138 Napoli, Italy. E-mail: arsenio.cutolo@unina.it

[5]Professor, Dept. of Civil, Environmental and Mechanical Engineering, Univ. of Trento, 38122 Trento, Italy; Center of Materials and Microsystems, Bruno Kessler Foundation, 38122 Trento, Italy; School of Engineering and Materials Science, Queen Mary Univ., London E1 4NS, U.K. E-mail: nicola.pugno@unitn.it

[6]Professor, Dept. of Civil, Environmental and Mechanical Engineering, Univ. of Trento, 38122 Trento, Italy; Division of Aerospace Engineering, Mechanical, Aerospace, and Civil Engineering, College of Engineering, Design and Physical Sciences, Brunel Univ. London, Uxbridge UB8 3PH, U.K.; Dept. of Nanomedicine, Houston Methodist Research Institute, Houston, TX 77030. E-mail: deseri@andrew.cmu.edu

Note. This manuscript was submitted on February 9, 2016; approved on August 9, 2016; published online on October 28, 2016. Discussion period open until March 28, 2017; separate discussions must be submitted for individual papers. This paper is part of the ***Journal of Engineering Mechanics***, © ASCE, ISSN 0733-9399.

also been experimentally observed that the response of cells to ultrasound strongly depends on the associated applied energy and on the related frequencies (Schuster et al. 2013). Furthermore, cell membrane damage was observed in leukemic blood cells and in blood cells after ultrasound treatment (Ellwart et al. 1988), with laboratory evidences showing that tumor cells were often more prone to be killed than healthy ones when exposed ultrasound (Lejbkowicz and Salzberg 1997; Lejbkowicz et al. 1993). Moreover, adequately modulated ultrasounds seem to be additionally capable of decreasing malignant cell growth, inhibiting cell proliferation (Chumakova et al. 2006; Honda et al. 2004), and stimulating or increasing wound healing (Schuster et al. 2013), although the authors of these works admit that "the molecular mechanism of ultrasound-induced apoptosis has not yet been clearly understood." In this framework, Mizrahi et al. (2012) have recently experimentally observed relevant dynamics involving cytoskeleton remodeling of human airway smooth muscle cells undergoing low-intensity ultrasounds administered both at small strains (10^{-5}) and ultrasonic frequencies (10^6 Hz) and at moderately large deformation regimes (10^{-1}) and low (physiological) frequencies (10^0 Hz).

Although describing the underlying mechanisms through which cells perceive and transduce mechanical vibrations is still a challenging task, theoretical studies (Fraldi et al. 2015; Or and Kimmel 2009) have recently explored the possibility that the relative displacement between cell organelles and cytoplasm induced by ultrasonic waves and caused by the different inertia of the media plays a key role in the resonancelike phenomena, suggesting that ultrasound (US)-induced mechanical oscillations greater than thermal maximal fluctuations can actually kindle strain regimes at high frequency and hence fatiguelike phenomena, thereby altering signaling pathways within the cell and thus inducing multimolecular complexes conformational shift or disrupting at critical frequencies found both approximately 45 and 1 MHz (Johns 2002).

The interest on the analysis of the in-frequency response of single-cell systems is further increased by some experimental studies performed in recent years on individual cancer and healthy cells of different types, which have demonstrated that the former were approximately 70% softer than the latter (Cross et al. 2008, 2007; Faria et al. 2008; Ketene et al. 2012; Lekka et al. 2012a, b, 1999; Li et al. 2008; Nikkhah et al. 2010; Prabhune et al. 2012; Rebelo et al. 2013), regardless of the cell lines examined and independently from the specific measurement technique used for determining the mechanical properties (e.g., atomic force microscopy and optical tweezers). These results could be in fact helpfully utilized, at least in principle, for mechanically targeting and selectively attacking cancer cells, leading to envisage possible new applications in diagnoses and therapies of cancer diseases (Fraldi et al. 2015; Jonieztz 2012).

Therefore, motivated by the aforementioned literature findings and aiming to enrich the modeling of single-cell systems, the present work investigated the effect of the prestress (for instance, induced in protein filaments during cell adhesion) on the overall cell stiffness, finally determining its influence on the in-frequency response of the cell. A simple multiscale scheme that incorporates finite elasticity is first proposed to include, by using a bottom-up homogenization procedure, suitable prestress-modified stiffness values into the viscoelastic single-cell models. Once the analytical expression of the overall elastic stiffness of an adherent cell has been obtained, some key model parameters (i.e., prestretch and number of "active" filaments) are identified and determined to fit the realistic stiffness moduli experimentally measured in the literature for several cell types. Finally, after a short presentation of new generalized spring-pot (fractional derivative–based) viscoelastic models, the role played by the stretched state of the cytoskeletal elements on the cell vibration is studied in detail through sensitivity analyses.

Elemental Nonlinear Elastic Model of Adherent Cell

Influence of Prestress and Number of Cytoskeleton Filaments on Single-Cell Stiffness

To derive the effect of the prestretch accumulated in the cytoskeleton filaments on the overall single-cell stiffness, this section presents a simple nonlinear elastic model of the cell structure, in which the essential features responsible for the mechanical response of the ensemble [e.g., cytoskeleton protein filaments, cell nucleus, and interface conditions with a rigid substrate, such as the extracellular matrix (ECM)] are taken into account, thus determining the cell elasticity through a bottom-up procedure.

Fig. 1 shows that, starting from a generally unknown initial stress-free configuration [Fig. 1(a)], the cell is assumed to be in an actual prestretched configuration [i.e., adherent to the ECM, as shown in Fig. 1(b)] and then subjected to a small displacement of its nucleus [Fig. 1(c)]. In this scheme, as highlighted in the lateral view (Fig. 1), the cell cytoskeleton is modeled through a structure made of symmetrically and radially placed nonlinear elastic filaments (or filament strands) anchored to the central nucleus and to the substrate through the focal adhesion points, thus implicitly assuming that the cell membrane follows the overall geometry of the model. Also, for the sake of simplicity, the entire kinematics is projected in the horizontal plane (i.e., the plane defined by the focal adhesion points), thereby neglecting the minor effects of stress and strain aliquots associated to the out-of-plane filament elongations caused by the cell stretching. In particular, a reference prestretch (denoted by λ_p) characterizes the deformed configuration in which the nucleus is constrained by n elastic strings (representing the actin filaments) arranged uniformly around the nucleus and identified by an angle $\phi_{j0} = j(2\pi/n)$.

To find how the cell structure influences the overall cell stiffness when its filaments are prestressed, by referencing a small-on-large approach, the nucleus is displaced of u in an arbitrary (e.g., horizontal) direction: as a consequence, maintaining prescribed the focal adhesion points, each filament will result to be stressed to follow the nucleus, and the corresponding Piola-Kirchhoff stress tensor can be generally written as

$$\mathbf{P}_j = \begin{pmatrix} P_{Lj} & 0 & 0 \\ 0 & P_{Tj} & 0 \\ 0 & 0 & P_{Tj} \end{pmatrix} \tag{1}$$

where, for the jth filament, P_{Lj} = longitudinal stress component and P_{Tj} = transverse stress component, which in this case is to be set equal to zero. Once the force f_u to be applied to the nucleus for obtaining the displacement u is determined, the related equivalent tangent stiffness can be formally derived as follows:

$$K_{\text{eq}} = \left.\frac{\partial f_u}{\partial u}\right|_{u=0} \tag{2}$$

Obviously, the force f_u [the resultant of the axial forces of the n filaments (Fig. 2)] will depend on u, the prestretch λ_p of each single filament, the initial stiffness (related to the stress-free configuration), the geometrical parameters, the number n of filaments, and the constitutive assumption, for example, the type of hyperelastic law chosen for the strings. Therefore, one has

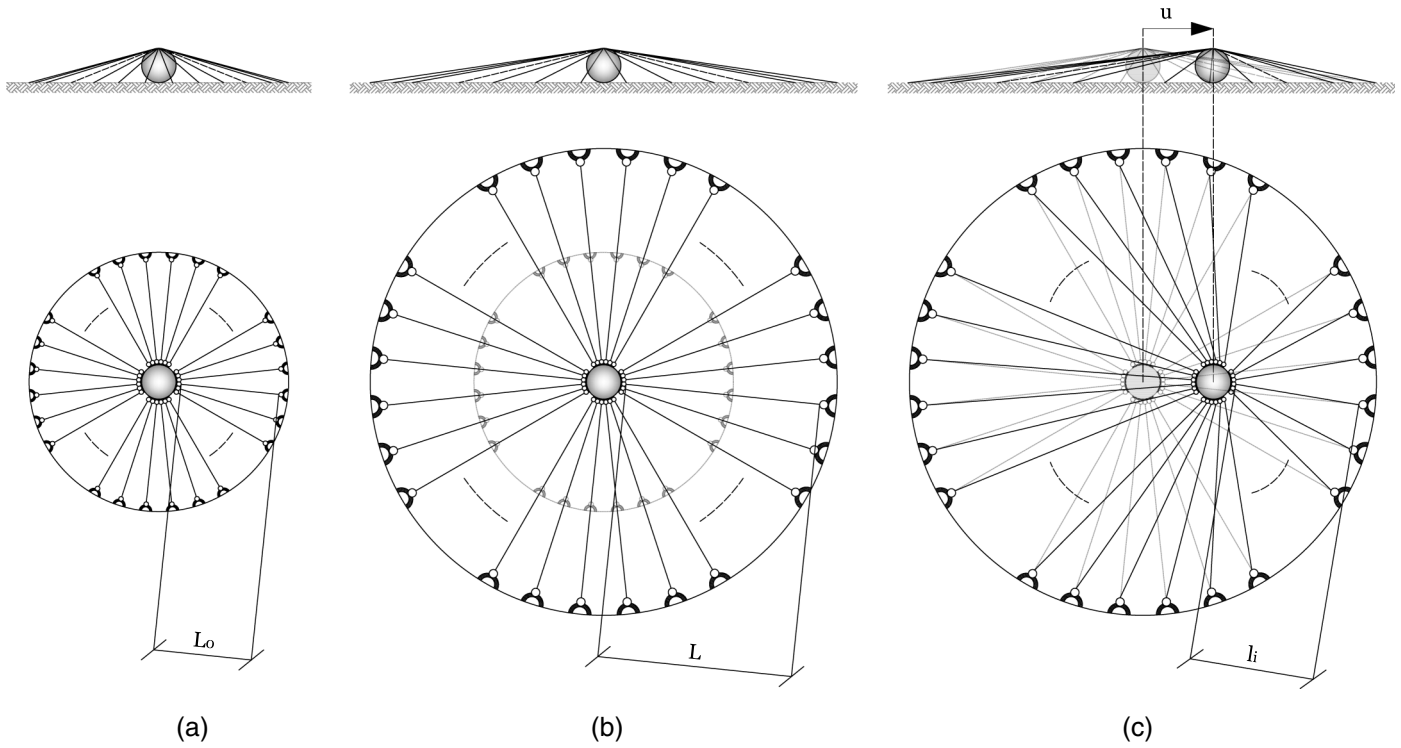

Fig. 1. Plan and lateral views of the elemental cell cytoskeleton structure: (a) initial (stress-free) unknown configuration; (b) adherent cell with nonlinearly prestretched/prestressed filaments (reference configuration); (c) small-on-large cell deformation induced by nucleus displacement (current configuration)

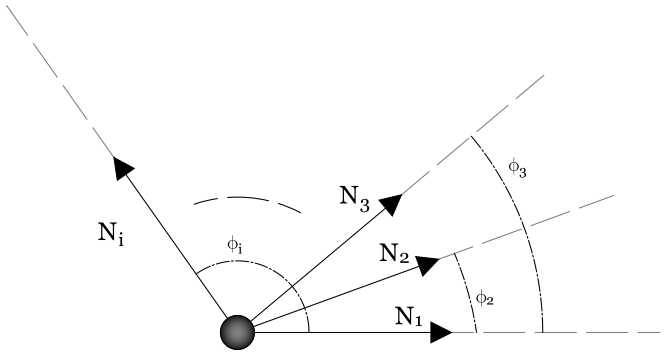

Fig. 2. How the axial forces kindled in each string contribute to the equilibrium of the nucleus; ϕ_j angles are referred to the actual (displaced) nucleus position

$$f_u + \sum_{j=1}^{n} N_j \cos(\phi_j) = 0 \tag{3}$$

where $N_j = P_{Lj}A$ = contribution of the jth filament attributed to the longitudinal stress times the reference cross-section area $A = A_j$ and ϕ_j = angle of the jth filament in its current configuration.

The constitutive model for the strings is fixed by following Holzapfel (2000), in the case of compressible Neo-Hookean solids in which the strain energy density function (SEDF) is written in terms of the first invariant, I_1, of the right Cauchy-Green tensor $\mathbf{C} = \mathbf{F}^{\mathbf{T}}\mathbf{F}$ (chosen as measure of the deformation), which in the so-called coupled form—in which the isochoric and volumetric parts are interacting—is given by

$$\Psi_{\mathrm{NH}} = \frac{G}{2}(I_1 - 3) + \frac{G}{2\beta}(J^{-2\beta} - 1) \quad \text{with } \beta = \frac{\nu}{1-2\nu} \tag{4}$$

where $J = \det \mathbf{F}$; and G and ν = shear modulus and the Poisson's ratio, respectively. The principal stresses will hence depend on the principal stretches in the form

$$P_j = \frac{\partial \Psi_{\mathrm{NH}}}{\partial \lambda_j} \tag{5}$$

and

$$P_{Lj} = G\left[\lambda_{Lj} - \frac{(\lambda_{Lj}\lambda_{Tj}^2)^{2\nu/2\nu-1}}{\lambda_{Lj}}\right] \tag{6}$$

$$P_{Tj} = 2G\left[\lambda_{Tj} - \frac{(\lambda_{Lj}\lambda_{Tj}^2)^{2\nu/2\nu-1}}{\lambda_{Tj}}\right] \tag{7}$$

Algebraic manipulations reveal that prescribing uniaxial stress states in each filament ($P_{Tj} = 0$) reduces to impose $\lambda_T = \lambda_L^{-\nu}$, finally obtaining the longitudinal stress as follows:

$$P_{Lj} = G\lambda_{Lj}[1 - \lambda_{Lj}^{-2(1+\nu)}] \tag{8}$$

The total stretch in the generic jth filament strand can be multiplicatively written as

$$\lambda_{Lj} = \lambda_p \lambda_{uj} \tag{9}$$

where $\lambda_p = L/L_0$ = initial prestretch related to the current filament length L referred to the initial configuration L_0, whose values are in this paper assumed to be the same for all the elements because of

the symmetry of the initial cell shape; and λ_{uj} = stretch of the jth string caused by the displacement u and explicitly given by

$$\lambda_{uj} = \frac{\sqrt{L^2 \sin^2 \phi_j + (L \cos \phi_j - u)^2}}{L} \tag{10}$$

where

$$\sin \phi_j = \frac{L \sin \phi_{j0}}{\sqrt{L^2 \sin^2 \phi_{j0} + (L \cos \phi_{j0} - u)^2}},$$
$$\cos \phi_j = \frac{L \cos \phi_{j0} - u}{\sqrt{L^2 \sin^2 \phi_{j0} + (L \cos \phi_{j0} - u)^2}} \tag{11}$$

Finally, by substituting Eqs. (8) and (3) into Eq. (2), after some further algebraic manipulations, the stiffness K is obtained, which varies with the displacement u as follows:

$$K = -GA\lambda_p \sum_{j=1}^{n} \left\{ \left[1 + (1+2\nu)\lambda_p^{-(1+2\nu)} \lambda_{uj}^{-2(1+\nu)} \right] \cos \phi_j \frac{\partial \lambda_{uj}}{\partial u} \right.$$
$$\left. - \left(\lambda_{uj} - \lambda_p^{-2(1+\nu)} \lambda_{uj}^{-(1+2\nu)} \right) \sin \phi_j \frac{\partial \phi_j}{\partial u} \right\} \tag{12}$$

from which one finally has

$$K_{\text{eq}} = K|_{u=0}$$
$$= GAL^{-1} \lambda_p \sum_{j=1}^{n} \{ 1 + \lambda_p^{-2(1+\nu)} [\nu + (1+\nu) \cos 2\phi_{j0}] \} \tag{13}$$

which represents the analytical form—explicitly depending on both the geometrical and mechanical parameters—of the tangent stiffness of the adherent single-cell structure, associated with the imposed displacement u. From Eq. (13) and for an arbitrary couple of filaments with prescribed angles ϕ_{j0} and $\phi_{j0} + \pi$, respectively, the prestretch influences the stiffness in a nonlinear way, whose form depends on Poisson's ratio ν. It is then natural to ask whether the stiffness is monotonic with the prestretch. By calculating the derivative of the jth addend (and its coaxial) in K_{eq}, that is, K_{eqj}, with respect to λ_p and equating it to zero, one finds

$$\frac{\partial K_{\text{eqj}}}{\partial \lambda_p} = GAL^{-1} \cos \phi_{j0} \lambda_p \left[1 + (1+2\nu) \lambda_p^{-2(1+\nu)} \right] = 0 \tag{14}$$

whose closed-form solution is

$$\lambda_p = |1 + 2\nu|^{1/1+\nu} \tag{15}$$

which gives compatible (positive) stretches for any angle ϕ_{j0} and Poisson's ratios belonging to the classical thermodynamically consistent range $]-1, 1/2[$.

From the biomechanical point of view, this counterintuitive result implies that, as the stiffness varies with increasing prestretches, a minimum must be found (Fig. 3); thus, at least in principle, during a monotonic stretching of the substrate or in searching optimal cytoskeleton configuration, an adherent cell could find minimal energy positions at nonzero strains as well.

Identification of Model Parameters to Describe Actual Cell Stiffness

The aforementioned nonlinear elastic model has been introduced to quantitatively estimate the effect of prestress and number of filaments on the overall stiffness of an adherent (prestretched) single cell. With reference to the experimentally measured cell stiffness values [see for a synoptic frame the tables in Fraldi et al. (2015)] and by using Eq. (13), it is possible to determine the equivalent overall elastic Young's modulus of the cell in an arbitrary prestretched configuration, E_{eq}, by considering an incompressibility condition, that is, $G \simeq E/3$, with G = first Lamé modulus, as follows ($C_{0G} = 6\pi GR$ will be used afterward for the stiffness):

$$E_{\text{eq}} \simeq \frac{3K_{\text{eq}}}{6\pi R} \tag{16}$$

where R = cell nucleus radius, as reported by Or and Kimmel (2009). This expression, which will be used in the following viscoelastic schemes, implicitly takes into account the prestretch and the number of filaments, all these parameters being included in K_{eq}. As a consequence, the formula furnishes a direct first estimation of the equivalent cell Young's modulus E_{eq} once all the mechanical and geometrical parameters are known. However, because of its elementary structure, it can be also used to identify the number of "active" cytoskeleton elements in an experimental measurement and to determine the average prestress of an adherent cell.

Fig. 4 illustrates the results of the parametric analyses conducted on the equivalent stiffness for three values of the Poisson's ratio of the filaments ($\nu = 0$, 0.25, 0.5), initial filament length $L_0 = 50$ μm, and circular cross sections with diameters of 7 nm, all these values being coherent with the literature. In particular, the equivalent cell Young's moduli of a cell have been carried out by both considering 75 active protein filaments for a single cell strand, varying the prestretch [Fig. 4(a)], and complementarily prescribing a prestretch ($\lambda_p = 1.3$), thus plotting the cell stiffness against the number of filaments [Fig. 4(b)]. Both the graphics show how the whole range of elastic moduli measured through different techniques and reported in the literature for a vast class of cell lines (Fraldi et al. 2015) can be obtained with good agreement, modulating the prestretch and the number of active filaments within experimentally documented intervals. An instructive numerical example can be easily done by considering the case of cell stiffness measured by Cross et al. (2008) for human healthy cells and corresponding abnormal carcinoma of the lung, estimated as approximately 2,100 and 560 Pa, respectively. In this case, setting $\nu = 0.4$, the stiffer value associated with the healthy cells can be obtained through the proposed model by assuming a prestretch

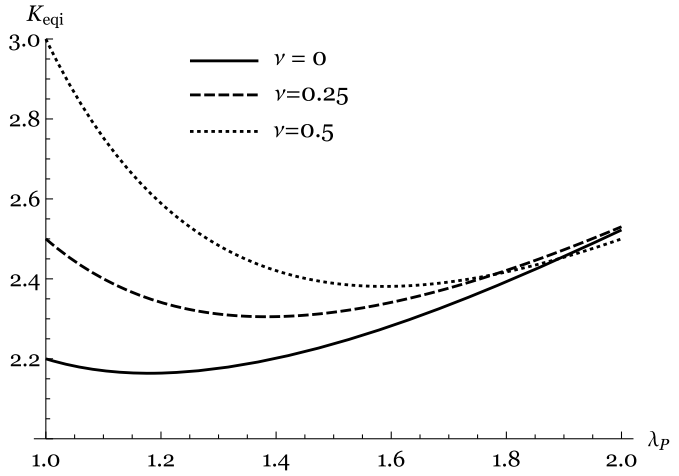

Fig. 3. Dimensionless contribution of a filament to the cell stiffness as function of the prestretch; for different Poisson's ratio values, a minimum is always highlighted

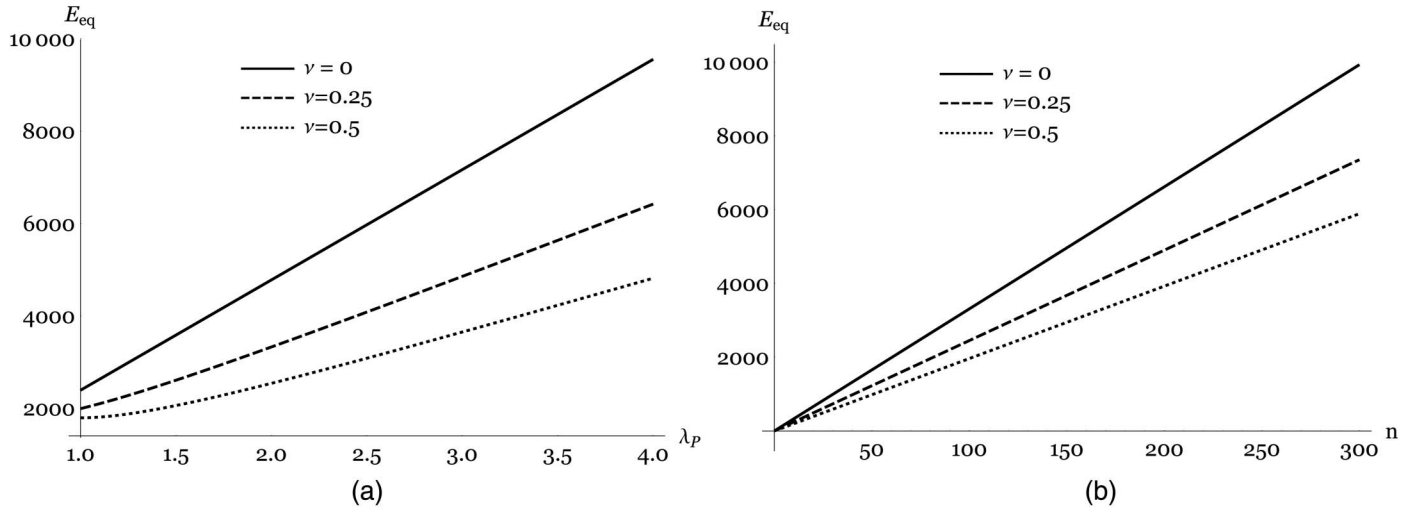

Fig. 4. Parametric analyses for the equivalent Young's modulus of a single-cell system for different Poisson's ratios: (a) elastic stiffness versus prestretch with fixed number of active filaments (75); (b) elastic stiffness versus number of (active) filaments, with prescribed prestretch value ($\lambda_p = 1.3$)

of $\lambda_p = 1.32$ and considering $n = 75$ active protein filaments, the cancer cell elastic modulus being caught by merely reducing to approximately 26 the number of active filaments to simulate possible lower levels of polymerization in the cytoskeleton structure of cancer cells to facilitate squeezing and metastatic migration abilities.

In-Frequency Response of Adherent Single-Cell Viscoelastic Systems Incorporating Cytoskeleton Prestress

By exploiting the results obtained in the previous sections regarding the effects of the prestretched/prestressed cytoskeleton filaments on the cell stiffness and by starting from an approach proposed by Or and Kimmel (2009) and recently further developed by Fraldi et al. (2015) to analyze the case of vibrating cell nucleus in a viscoelastic environment excited by low-intensity therapeutic ultrasound (LITUS), consider a single-cell system whose dynamics is reduced to an oscillating mass immersed in a viscoelastic medium (Fig. 5). To represent the nucleus, a rigid sphere of radius R is thus considered by ideally concentrating in it the entire mass of the cell and modeling the environment as a homogeneous and isotropic viscoelastic medium. Under these hypotheses, the whole cell dynamics is completely governed by one degree of freedom stimulated by a velocity law assumed in the following form:

$$v_m(t) = v_{m0} e^{-i\omega_0 t} \tag{17}$$

where v_m = velocity prescribed to the medium; v_{m0} = amplitude of the complex velocity phasor; $\omega_0 = 2\pi f$ = oscillations angular frequency; and f = measured frequency in hertz. According to the aforementioned studies, the motion can be described by the following:

$$f_m = m_{ob} a_{ob} = \frac{4}{3}\pi R^3 \rho_{ob} \frac{d^2 u_{ob}}{dt^2} = f_{ac} - f_{\text{res}} \tag{18}$$

where t = time; f_m = inertial force; m_{ob} = nucleus mass of density ρ_{ob}; u_{ob} = displacement; and f_{ac} = driving force that is kindled by the acoustic pressure gradients triggered by the ultrasound transducer in the system. In the case under analysis, the object is very small compared with the acoustic wavelength; thus, the form of the acoustic force can be simply reduced to a force that ideally would act on a sphere of the same radius in the absence of the object (Maxey and Riley 1983). This permits

$$f_{ac} = \frac{4}{3}\pi \rho_m R^3 \frac{Dv_m}{Dt} \equiv \frac{4}{3}\pi \rho_m R^3 \frac{dv_m}{dt} \tag{19}$$

where ρ_m = density of the medium. Additionally, dimensional analyses show that the convective term is small; as a result, the absence of spatial variability allows to adopt in Eq. (19) time differentiation d/dt instead of the substantial derivative D/Dt (Or and Kimmel 2009). Also, f_{res} represents the response force applied to the object by its surrounding, attributed to their relative motion, and will thus depend on the overall rheological features of the environment. To catch possible further insights on the single-cell behavior, this force incorporates in a parametric way key geometrical and mechanical properties of interest.

The analyses will be performed by first using two quasi-standard viscoelastic models (Voigt and Maxwell) and then introducing a generalized standard linear Kelvin model, in which dashpot and spring elements are replaced by so-called spring-pot systems, which have been recently used in different ways to describe with success the mechanical behavior of biological materials (Deseri et al. 2013).

Additionally, by recalling the well-known relationship between Laplace and Fourier transforms (i.e., $\mathcal{F}[\cdot] = \mathcal{L}[\cdot]|_{s=i\omega}$), the Laplace transform is used in what follows to solve the differential problem at hand, thus obtaining the response of the systems directly in terms of frequency (Fraldi et al. 2015).

With respect to the assigned initial conditions, in all the simulations, the single-cell system is assumed to be initially at rest, that is

$$u_{ob}|_{t=0} = 0, \quad \left.\frac{du_{ob}}{dt}\right|_{t=0} = 0 \tag{20}$$

With Laplace transforming Eq. (18), one finally obtains

$$F_m = \frac{4}{3}\pi R^3 \rho_{ob} s^2 U_{ob} = F_{ac} - F_{\text{res}} \tag{21}$$

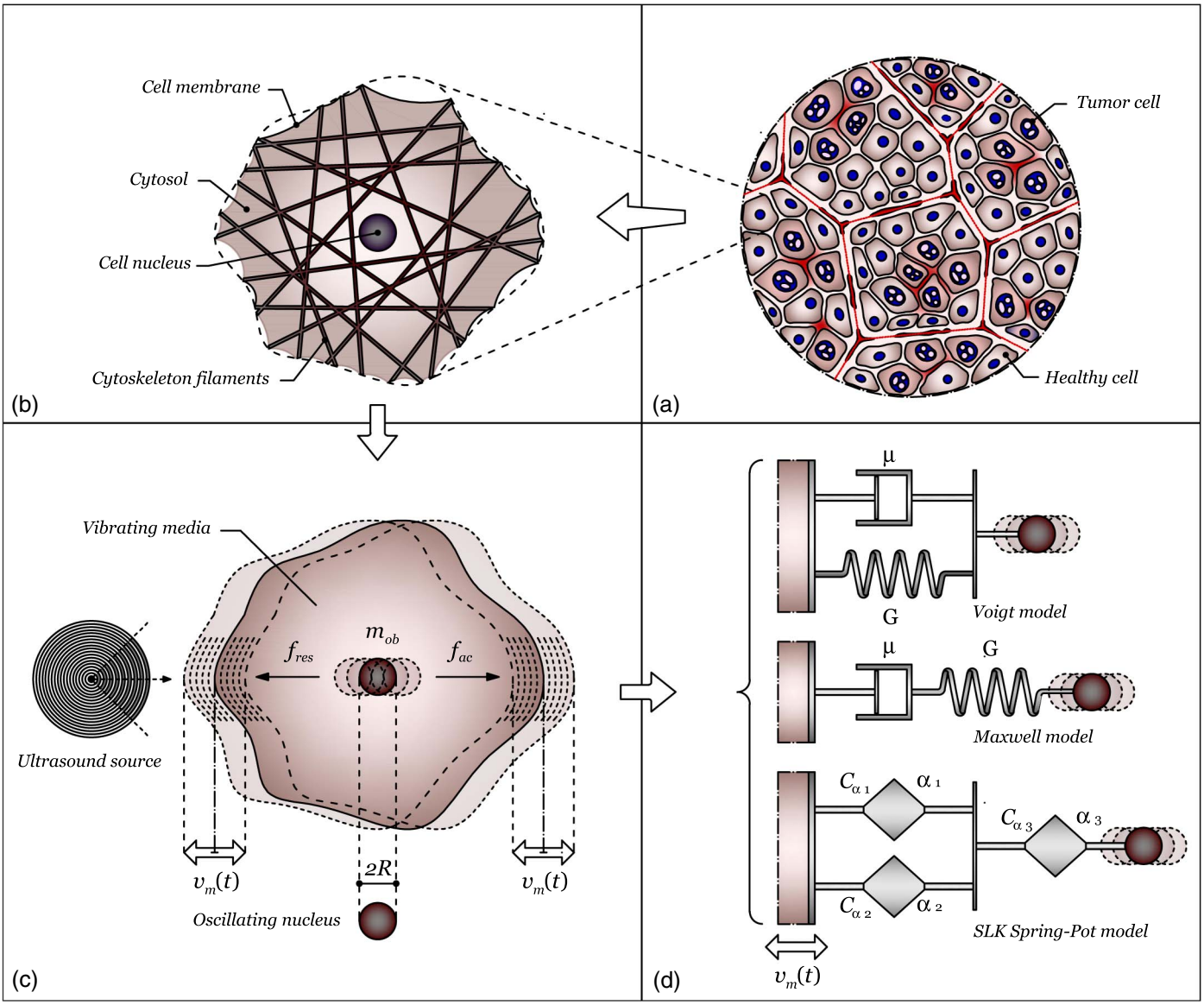

Fig. 5. Idealized single-cell system: (a) healthy and tumor cells agglomerate; (b) typical cell unit, with nucleus and cytoskeleton structure embedded in the cytosol and confined by the lipid bilayer cell membrane; (c) idealized single-cell system, with cell nucleus oscillating in a viscoelastic environment under the action of radiating ultrasound source; (d) adopted viscoelastic schemes (Voigt, Maxwell, and generalized spring-pot-based SLK models)

where s = Laplace variable and capital letters = Laplace-transformed terms. Accordingly, F_{ac} = Laplace transforming of the acoustic force f_{ac} reported in the Eq. (19), thus obtaining

$$F_{ac} = \frac{4}{3}\pi\rho_m R^3 s V_m = \frac{4}{3}\pi\rho_m R^3 s^2 U_m \tag{22}$$

Further details on the subsequently presented viscoelastic models are available in Fraldi et al. (2015).

Enhanced Voigt and Maxwell Models for Single Cells

The Voigt idealization assumes that viscous and elastic elements are placed in parallel with each other (Fig. 5). In this way, the resulting overall force can be determined by the simple sum of the forces attributed to the single constituting elements as

$$f_{\text{res}} = f_\mu + f_G \tag{23}$$

where f_μ = viscous contribution and f_G = elastic response. In case of a rigid object rapidly vibrating in viscous fluids, the viscous term can be helpfully represented with the following explicit form, as suggested by Basset (1888), Landau and Lifshitz (1987), and Or and Kimmel (2009):

$$f_\mu = 6\pi R\mu\left(1+\sqrt{\frac{\omega R^2}{2\eta}}\right)(v_{ob}-v_m) + \frac{2}{3p}\pi R^3\rho_m\left(1+\frac{9p}{2}\sqrt{\frac{2\eta}{\omega R^2}}\right)(\dot{v}_{ob}-\dot{v}_m) \tag{24}$$

where η and μ = kinematic and dynamic medium viscosities, respectively; and $v = \dot{u}$ = velocity. In Eq. (24), the structure of the viscous force is different from that of the standard Stokes, with frequency-dependent terms and an inertial (spurious) contribution

$3\pi R^3\rho_m\sqrt{2\eta/\omega R^2}$, named added mass (Brennen 1982), additionally appearing and p (in this equation, $p = 2$) being the number of elements in parallel introduced ad hoc in Fraldi et al. (2015) to solve an ambiguous situation already pointed out by Or and Kimmel (2009). In fact, as already highlighted in Fraldi et al. (2015), to avoid contrived solutions to remove "the excessive added-mass term" that "erroneously twice appears" in Or and Kimmel (2009), the viscoelastic forces are in this equation set to ensure that any combined viscoelastic scheme derived from the general fractional-based standard linear Kelvin (SLK) model contains the sole added-mass and virtual-friction contributions to be considered.

Following Ilinskii et al. (2005), the elastic force f_G can be given by

$$f_G = 6\pi GR(u_{ob} - u_m) + 6\pi R^2\sqrt{G\rho_m}(\dot{u}_{ob} - \dot{u}_m) + \frac{2}{3p}\pi R^3\rho_m(\ddot{u}_{ob} - \ddot{u}_m) \tag{25}$$

Similar to the viscous force, the elastic contribution in Eq. (25) is presented in a somehow enhanced version, with respect to the standard Hooke law, to include key effects of the cell nucleus–environment dynamic interactions, which characterize the actual physical behavior of the overall system attributed to rapid fluctuations. In Eq. (25), the physics is then caught through two additional dissipative and inertial terms, respectively, equal to $6\pi R^2\sqrt{G\rho_m}$ (the virtual friction) and the so-called added mass, with G representing the first Lamé modulus, and u_m the vibrational displacement of the medium. Also, for convenience, it is assumed that

$$c_{0G} = 6\pi GR, \quad c_{1G} = 6\pi R^2\sqrt{G\rho_m}, \quad c_{2G} = \frac{2}{3p}\pi R^3\rho_m \tag{26}$$

$$c_{1\mu} = 6\pi R\mu\left(1 + \sqrt{\frac{\omega R^2}{2\eta}}\right), \quad c_{2\mu} = \frac{2}{3p}\pi R^3\rho_m\left(1 + \frac{9p}{2}\sqrt{\frac{2\eta}{\omega R^2}}\right) \tag{27}$$

and a further dimensionless parameter is

$$\zeta = \frac{\rho_{ob}}{\rho_m} = \frac{1}{1+\gamma} \tag{28}$$

where $\gamma = \rho_m\rho_{ob}^{-1} - 1$. The modified Voigt viscoelastic equation is obtained as

$$f_{\text{res}} = c_{0G}(u_{ob} - u_m) + (c_{1\mu} + c_{1G})(\dot{u}_{ob} - \dot{u}_m) + (c_{2\mu} + c_{2G})(\ddot{u}_{ob} - \ddot{u}_m) \tag{29}$$

from which, by Laplace transforming, one finally has

$$F_{\text{res}} = (U_{ob} - U_m)[c_{0G} + (c_{1\mu} + c_{1G})s + (c_{2\mu} + c_{2G})s^2] \tag{30}$$

and, replacing Eqs. (30) and (22) in Eq. (21) and after some algebraic passages, the following equation is found:

$$\left\{c_{0G} + (c_{1\mu} + c_{1G})s + \left[(c_{2\mu} + c_{2G}) + \frac{4}{3}\pi\rho_{ob}R^3\right]s^2\right\}\Delta U = \frac{4}{3}\pi\gamma\rho_{ob}R^3sV_m \tag{31}$$

where $\Delta U = U_{ob} - U_m$. By solving Eq. (31), the analytical solution of the in-frequency response of the system, in terms of relative displacement ΔU of the cell nucleus with respect to the envinronment, is obtained in the form

$$|\Delta U|\Big|_{s=i\omega} = \left|\frac{\frac{4}{3}\pi\gamma\zeta\rho_m R^3 sV_m}{c_{0G} + (c_{1\mu} + c_{1G})s + [(c_{2\mu} + c_{2G} + \frac{4}{3}\pi\rho_{ob}R^3)]s^2}\right|\Bigg|_{s=i\omega} \tag{32}$$

Complementary to the case of Voigt, Maxwell systems present elastic and viscous elements ideally placed in series (Fig. 5). The overall response is therefore found by imposing the following isostress condition:

$$F_G = F_\mu = F_{\text{res}} \tag{33}$$

thus equating the sum of the viscous and the elastic displacement contributions to the total relative displacement, that is

$$\Delta U = \Delta U_G + \Delta U_\mu \tag{34}$$

where F_G and F_μ = Laplace transforms of the elastic and viscous forces given in Eqs. (25) and (24), respectively, thus obtaining

$$F_G = (c_{0G} + c_{1G}s + c_{2G}s^2)\Delta U_G, \quad F_\mu = (c_{1\mu}s + c_{2\mu}s^2)\Delta U_\mu \tag{35}$$

from which the elastic and viscous displacements can be explicitly written as

$$\Delta U_G = \frac{F_G}{c_{0G} + c_{1G}s + c_{2G}s^2}, \qquad \Delta U_\mu = \frac{F_\mu}{c_{1\mu}s + c_{2\mu}s^2} \tag{36}$$

By recalling F_{res} from Eq. (21) and considering Eq. (36), the closed-form solution for the in-frequency response of the enhanced Maxwell system is found as

$$|\Delta U|\Big|_{s=i\omega} = \left|\frac{\frac{4}{3}\pi\gamma\rho_{ob}R^3sV_m}{1 + \frac{4}{3}\pi\rho_{ob}R^3s^2\left(\frac{1}{c_{1\mu}s + c_{2\mu}s^2} + \frac{1}{c_{0G} + c_{1G}s + c_{2G}s^2}\right)}\right|\Bigg|_{s=i\omega} \tag{37}$$

Single-Cell Response through Generalized Fractional Derivative–Based Standard Linear Kelvin Paradigms

Added Mass and Virtual Friction in Spring-Pot Models

In a viscoelastic medium using fractional derivatives, the mechanical behavior is interpreted through the introduction of spring-pot systems. The first time that the fractional derivative concept is traced in an epistolary correspondence between de L'Hopital and Leibniz dates back to 1695 (Podlubny 1999), in which they tried to answer the following question: "What does the derivative $d^n f(x)/dx^n$ mean if $n = 1/2$?" Since that time, a new branch of mathematics—fractional calculus, a generalization of the commonly used integer-order differentiation and integration—has been formally developed. The basic idea, as suggested by Riemann-Liouville, is in fact to interpret the fractional derivative as the inverse operation of a fractional integral. The use of fractional derivatives in viscoelasticity can be traced in the work by Nutting (1921), in which, from the best fitting of experimental curves, he noted the possibility of describing the relationship between deformation and time through a power law, that is, $u \propto t^n F^m$, in which F = force; and u = displacement. In 1949, Blair and Caffyn (2010) analytically justified this experimental curve by using the fractional derivatives and also introducing the spring-pot model. Afterward, Caputo (1969) in detail proposed a fractional derivative operator, namely, ${}_a^C D_t^\alpha$, which could be used in the real world:

$$ {}_a^C D_t^\alpha f(t) = \frac{1}{\Gamma(n-a)} \int_a^t (t-s)^{n-\alpha-1} f^n(s) ds \quad \forall\ n-1 \le \alpha \le n \tag{38} $$

where Γ = Euler gamma function and $f(t)$ = integrable in $[a, t]$.

In recent years, several scientific papers involving fractional calculus–based viscoelasticity has been presented, for both approaching standard problems and analysing complex systems in pioneering physical and engineering fields (e.g., Atanackovic et al. 2007; Bagley 1983; Deseri et al. 2013, 2014; Di Paola et al. 2009, 2013; Grillo et al. 2015; Mainardi 2012; Metzler and Klafter 2000; Schiessel and Blumen 1993). For the present purpose, however, the spring-pot model is essentially that first proposed by Blair and Caffyn (2010), which is generalized ad hoc in this paper to integrate added mass and virtual friction as additional system features. Hence, the following definition of the spring-pot response force f_{SP} is introduced:

$$ f_{\mathrm{SP}} \coloneqq C_\alpha [{}_0^C D_t^\alpha (u_{ob} - u_m)] + c_{1\mathrm{SP}} (\dot{u}_{ob} - \dot{u}_m) + c_{2\mathrm{SP}} (\ddot{u}_{ob} - \ddot{u}_m) \tag{39} $$

in which ${}_0^C D_t^\alpha$ = Caputo's fractional time-derivative of order α [$\alpha \in [0, 1]$ being over the time interval $(0, t)$]; and C_α = suitable frequency-dependent parameter written by starting from Koeller (1984) as follows:

$$ C_\alpha = c_{0G} \left(\frac{c_{1\mu}}{c_{0G}} \right)^\alpha \tag{40} $$

In particular, dissipative and inertial terms were incorporated in the model by postulating the simplest mathematical structure

$$ c_{1\mathrm{SP}} = (1-\alpha) c_{1G}, \qquad c_{2\mathrm{SP}} = c_{2G} \left(1 + \alpha \frac{9p}{2} \sqrt{\frac{2\eta}{\omega R^2}} \right) \tag{41} $$

thereby reproducing the elastic and viscous models proposed by Or and Kimmel (2009) as special limit cases, that is, $\alpha = 0$ and $\alpha = 1$, respectively.

By substituting Eq. (39) into Eq. (21) and invoking the fractional derivative rule allowing to Laplace transform by preserving the classical (integer) derivative law for the Laplace variable s, namely, ${}_0^C D_t^\alpha \xrightarrow{\mathcal{L}} s^\alpha$, the in-frequency response of the spring-pot model, in terms of nucleus-environment relative displacement, can be finally found in the following form:

$\forall\ \alpha \in [0, 1]$,

$$ |\Delta U|\Big|_{s=i\omega} = \left| \frac{\frac{4}{3}\pi\gamma\rho_{ob} R^3 s V_m}{\left(\frac{4}{3}\pi\rho_{ob} R^3 + c_{2\mathrm{SP}}\right) s^2 + c_{1\mathrm{SP}} s + C_\alpha s^\alpha} \right| \Bigg|_{s=i\omega} \tag{42} $$

Generalized SLK Model Incorporating Spring-Pot Systems

To enrich Maxwell and Voigt viscoelastic behaviors, different standard linear solid (SLS) systems can be encountered in the literature (Tschoegl 1989). Among these, one of the most used scheme is composed of the SLK model, obtained by placing in series an elastic spring with a Voigt system; the Maxwell-Wiechert model, representing an alternative and somehow complementary configuration in which an elastic spring is positioned in parallel with a Maxwell system, whose multielement version leads to the well-known Prony series method.

Given that the spring pot might be physically interpreted as a viscoelastic system intrinsically capable to smoothly generate intermediate mechanical responses as the aforementioned parameter α moves from zero to one in the limit cases giving purely elastic and viscous behaviors, respectively, a possible generalization of the SLK model can be envisaged by replacing in it each dashpot and spring with a spring pot, as shown in Fig. 5, by further enhancing the resulting model by suitably including added-mass and virtual-friction terms. In this way, a powerful (linear) low-parameter viscoelastic system can be realized with the important advantage that, by essentially following the aforementioned proposed strategies, the analytical solutions of the corresponding in-frequency system response can be always derived for any modulation and combination of the spring-pot parameter α. As a result, a wide range of otherwise unforeseeable viscoelstaic responses can be caught, and all the simpler viscoelastic models and the related analytical solutions recalled previously, including those of Or and Kimmel (2009), can be obtained as special limit cases of the proposed generalized SLK scheme as well.

With reference to the configuration of the spring pot in the proposed generalized SLK viscoelastic system (Fig. 5), equilibrium among forces and compatibility for the displacements may be written as

$$ f_{\mathrm{SLK}} = f_P = f_{\mathrm{SP3}} \tag{43} $$

$$ \Delta u_{\mathrm{SLK}} = \Delta u_P + \Delta u_{\mathrm{SP3}} \tag{44} $$

where f_{SLK} = total force; $f_P = f_{\mathrm{SP1}} + f_{\mathrm{SP2}}$; f_{SP1}, f_{SP2}, and f_{SP3} = single contributions given by the three spring pots whose explicit forms are furnished by Eq. (39); and the displacement $\Delta u_P = \Delta u_{\mathrm{SP1}} = \Delta u_{\mathrm{SP2}}$.

By Laplace transforming f_P and f_{SP3}, the fractional derivative rule ${}_0^C D_t^\alpha \xrightarrow{\mathcal{L}} s^\alpha$ gives

$$ F_P = [C_{\alpha 1} s^{\alpha 1} + C_{\alpha 2} s^{\alpha 2} + (c_{1\mathrm{SP1}} + c_{1\mathrm{SP2}}) s + (c_{2\mathrm{SP1}} + c_{2\mathrm{SP2}}) s^2] \Delta U_P \tag{45} $$

$$ F_{\mathrm{SP3}} = [C_{\alpha 3} s^{\alpha 3} + c_{1\mathrm{SP3}} s + c_{2\mathrm{SP3}} s^2] \Delta U_{\mathrm{SP3}} \tag{46} $$

Algebraic manipulations allow

$$ \Delta U_P = \frac{F_P}{C_{\alpha 1} s^{\alpha 1} + C_{\alpha 2} s^{\alpha 2} + (c_{1\mathrm{SP1}} + c_{1\mathrm{SP2}}) s + (c_{2\mathrm{SP1}} + c_{2\mathrm{SP2}}) s^2} \tag{47} $$

$$ \Delta U_{\mathrm{SP3}} = \frac{F_{\mathrm{SP3}}}{C_{\alpha 3} s^{\alpha 3} + c_{1\mathrm{SP3}} s + c_{2\mathrm{SP3}} s^2} \tag{48} $$

Therefore, by recalling the previously obtained relationship for F_{res}, the closed-form in-frequency solution for the SLK system is finally determined as

$$ |\Delta U_{\mathrm{SLK}}|\Big|_{s=i\omega} = \left| \frac{\frac{4}{3}\pi\gamma\rho_{ob} R^3 s V_m \left[\frac{1}{s(c_{1\mathrm{SP1}} + c_{1\mathrm{SP2}}) + s^2 (c_{2\mathrm{SP1}} + c_{2\mathrm{SP2}}) + C_{\alpha 1} s^{\alpha 1} + C_{\alpha 2} s^{\alpha 2}} + \frac{1}{s(c_{1\mathrm{SP3}} + c_{2\mathrm{SP3}} s) C_{\alpha 3} s^{\alpha 3}} \right]}{\frac{4}{3}\pi\rho_{ob} R^3 s^2 \left[\frac{1}{s(c_{1\mathrm{SP1}} + c_{1\mathrm{SP2}}) + s^2 (c_{2\mathrm{SP1}} + c_{2\mathrm{SP2}}) + C_{\alpha 1} s^{\alpha 1} + C_{\alpha 2} s^{\alpha 2}} + \frac{1}{s(c_{1\mathrm{SP3}} + c_{2\mathrm{SP3}} s) + C_{\alpha 3} s^{\alpha 3}} \right] - 1} \right| \Bigg|_{s=i\omega} \tag{49} $$

Table 1. Synoptic Table with Models and Adopted Parameters

Models	Parameters					
	α_1	C_{α_1}	α_2	C_{α_2}	α_3	C_{α_3}
Elastic	0	$\rightarrow\infty$	—	—	0	c_{0G}
Viscous	0	$\rightarrow\infty$	—	—	1	$c_{1\mu}$
V	0	c_{0G}	1	$c_{1\mu}$	0	$\rightarrow\infty$
M	0	$\rightarrow 0$	1	$c_{1\mu}$	0	c_{0G}
SLK	0	c_{0G}	1	$c_{1\mu}$	0	c_{0G}
SLK_1	0.5	$C_{0.5}$	1	$c_{1\mu}$	0	c_{0G}
SLK_2	0	c_{0G}	0.5	$C_{0.5}$	0	c_{0G}
SLK_3	0	c_{0G}	1	$c_{1\mu}$	0.5	$C_{0.5}$

This equation thus gives the analytical response of a generalized SLK model capable to cover a wide range of possible intermediate viscoelastic behaviors reproduced by tuning the fractional derivative order α characterizing the spring pots, and incorporating added-mass and virtual-friction effects (Fraldi et al. 2015) and replicating, as limit cases, all the simpler (viscous and elastic) and nonstandard single-cell literature models (Or and Kimmel 2009). Some systems obtained by modulating the parameters α in the proposed model are summarized in Table 1 with reference to selected cases afterward used for simulating the in-frequency response of single cells to mechanical loads (i.e., elastic; viscous; Voigt; Maxwell; SLK limit cases; and the three intermediate chosen configurations, namely, SLK_1, SLK_2, and SLK_3).

Resonance Hypothesis in Adherent Cells: Role of Prestretch and Number of Active Cytoskeleton Filaments

In a recent paper by some of the present authors (Fraldi et al. 2015), the in-frequency response of single-cell systems has been analyzed in detail through simple (one degree of freedom) viscoelastic schemes and by conducting sensitivity analyses to gain information about positioning and magnitude of the response peaks for envisaging possibilities of exploiting the stiffness discrepancies experimentally observed between healthy and tumor cells for mechanically targeting and selectively attacking cancer cells. Thus, the authors explored the in-frequency responses of a wide class of viscoelastic single-cell paradigms by introducing ad hoc a new generalized fractional derivative–based SLK model and constructing the related analytical solutions, whose results were considered ranges of mechanical properties and physical parameters actually measured at single-cell level and reported in the consolidated literature.

However, when dealing with living systems, the measures of stiffness can be significantly affected by intrinsic structural changes of the biological matter, for example, by the reorganization dynamics guided by polymerization-depolymerization processes, which change the internal configuration of the cytoskeleton, thereby regulating adhesion and migration cell capabilities and in turn provoking nonhomogeneous cell deformations and changes in stiffness (Bao and Suresh 2003; Brunner et al. 2009; Rodriguez et al. 2013), with Young's moduli also oscillating from approximately 100 Pa to 10 kPa (Caille et al. 2002; Cross et al. 2008, 2007; Faria et al. 2008; Ketene et al. 2012; Lekka et al. 2012a, b, 1999; Li et al. 2008; Nikkhah et al. 2010; Prabhune et al. 2012; Rebelo et al. 2013).

Nevertheless, the vast majority of the experimental data somewhat consider stiffness of "round" (suspended) cells and, to the authors' best knowledge, not much effort has been devoted, from the modeling standpoint, to mechanically relate the overall change of cell stiffness to its stretched configuration and to the average number of active/assembled cytoskeletal filaments.

Therefore, by starting from the experimental results in the literature and taking into account the ranges within which actual measured mechanical features of cells can oscillate, the overall stiffness, determined from the proposed elemental nonlinear elastic single-cell model, has been introduced into the fractional derivative–based SLK scheme. In this way, the viscoelastic behavior of the cell explicitly depends, among other geometrical and physical parameters, on the stiffness resulting from the number of active cytoskeletal filaments, their prestretch level caused by possible adherent configurations, and the round shape–associated cell Young's modulus, which is directly related to the cell line and to the cell (i.e., healthy or cancer) state.

To highlight the possibility of following the previously described strategy for representing the whole range of the experimentally measured single-cell mechanical properties in both suspended and adherent conditions and demonstrating that viscoelastic response peaks still fall within frequencies intervals of ultrasound, which would still preserve the possibility of selectively inducing resonancelike phenomena in cells (Fraldi et al. 2015), sensitivity analyses have been performed ad hoc by varying the overall intrinsic round-shaped cell Young's modulus, the prestretch and the number of active microfilaments, the cytosol viscosity, and the nucleus size being prescribed and set equal to average values, thereby covering the entire range of the mechanical data given in the literature for many cell lines investigated.

By essentially following data and methods already introduced in Fraldi et al. (2015) and with respect to the notations proposed for the generalized SLK viscoelastic systems, the analyses reported subsequently have been conducted by assuming a medium-vibration velocity magnitude of $v_{m0} = 0.12$ ms^{-1}, determined in case of plain progressive waves characterized by an acoustic intensity of 1 W cm^{-2} and an associated intensity of $I = 0.5\rho_m c v_{m0}^2$, where $c = 1{,}500$ ms^{-1} = speed of sound at room temperature (Lide et al. 2008) at which mass density of the medium has been also assumed to be coincident with that of water and that of the nucleus [as reported in Michelet-Habchi et al. (2005)] to be approximately 30% more dense than the environment.

More specifically, the performed analyses have been referred to six selected viscoelastic schemes, that is, the enhanced Voigt, Maxwell, and SLK schemes and three other generalized fractional derivative–based SLK models with spring pots in Positions 1, 2, and 3 with $\alpha = 0.5$ (Fig. 5), in all the cases also taking into account added-mass and virtual-friction effects. Additionally, the elastic modulus G appearing in the fractional derivative–based models implicitly takes into account the cell configuration (suspended and adherent) through prestretch and number of active filaments determined by Eqs. (13) and (16). The theoretical outcomes have been carried out by using the symbolic commercial code *Mathematica* (Wolfram 2003) in the calculations, and the results have been represented in the domain of the frequencies within the interval that is most interesting for biomedical applications, that is, 1 kHz $\leq f \leq$ 100 MHz. In particular, the main attention is paid to the in-frequency system responses plotted in terms of maximum relative displacement $|\Delta U|$, in the time domain representing the magnitude of relative oscillations between environment and cell nucleus, induced by ultrasound.

Figs. 6–8 collect the most relevant results from the analytical models: cell stiffness, prestrech intensity, and number of filaments have been assumed to vary within intervals compatible with experimental findings, keeping fixed the other complementary parameters, and choosing for them the most common values in the

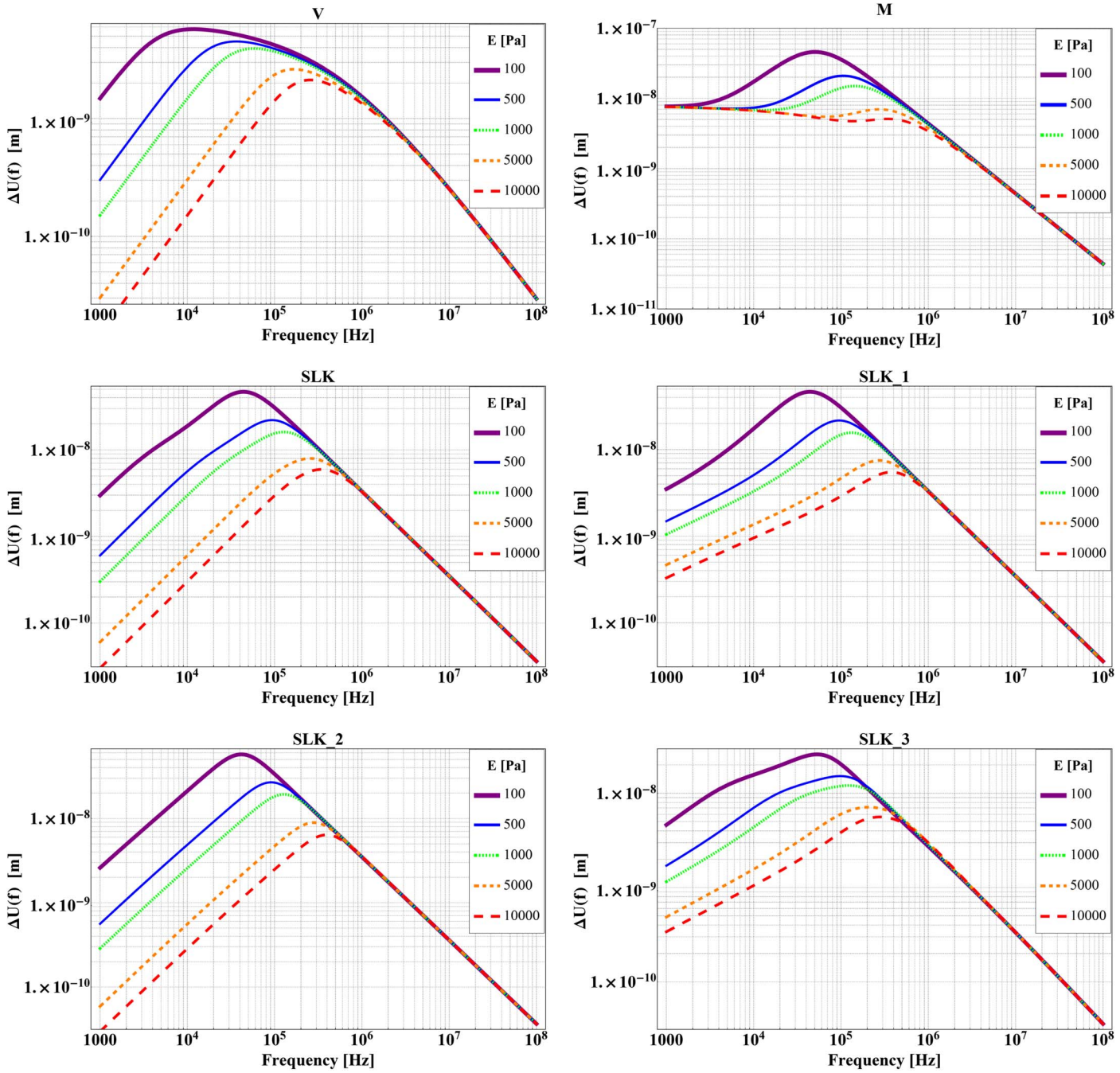

Fig. 6. Sensitivity analysis for the frequency response of the cyclic displacement amplitude of a spherical object ($R = 1$ μm) with respect to its surroundings, with prescribed viscosity ($\mu = 10^{-3}$ Pa · s) and varying Young's modulus ($E = 100$, 500, 1,000, 5,000, and 10,000 Pa); V = Voigt; M = Maxwell; and SLK_1, SLK_2, and SLK_3 = generalized SLK with spring pot in Positions 1, 2, and 3, respectively; $\alpha = 0.5$

literature, that is, Young's modulus of $E = 2{,}100$ Pa (Cross et al. 2007); cell nucleus radius of $R = 1$ μm (Cowin and Doty 2007); and water viscosity of $\mu = 10^{-3}$ Pa · s (Or and Kimmel 2009).

Fig. 6 particularly illustrates the cell in-frequency response in terms of relative displacement by parametrically varying the cell stiffness from $E = 100$ Pa to $E = 10$ kPa, coherently with data ranges reported in the experimental literature. Similarly, Figs. 7 and 8 show the results for the six viscoelastic models chosen by plotting displacement amplitude against frequency and respectively setting the tangent Young's modulus ($E = 2.6 \times 10^9$ Pa) and Poisson's ratio ($\nu = 0.4$) of the microfilaments, the viscosity $\mu = 10^{-3}$ Pa · s, and varying the prestretch λ_p and the number n of cytoskeleton filaments.

The outcomes obtained from the sensitivity analyses confirm both qualitative trends and quantitative results already found in Fraldi et al. (2015), with growing peak frequencies and associated decreasing displacement amplitudes as the overall cell stiffness grows up as a consequence of the increase of the intrinsic Young's moduli of the (round) cells (Fig. 6) and when the cell stiffening is induced by its adherent configuration, a situation in this paper modeled by increasing the tensile prestresses in the cytoskeletal elements and the number of prestretched filaments (Figs. 7 and 8). Also, in all the analyzed single-cell systems, the results highlight

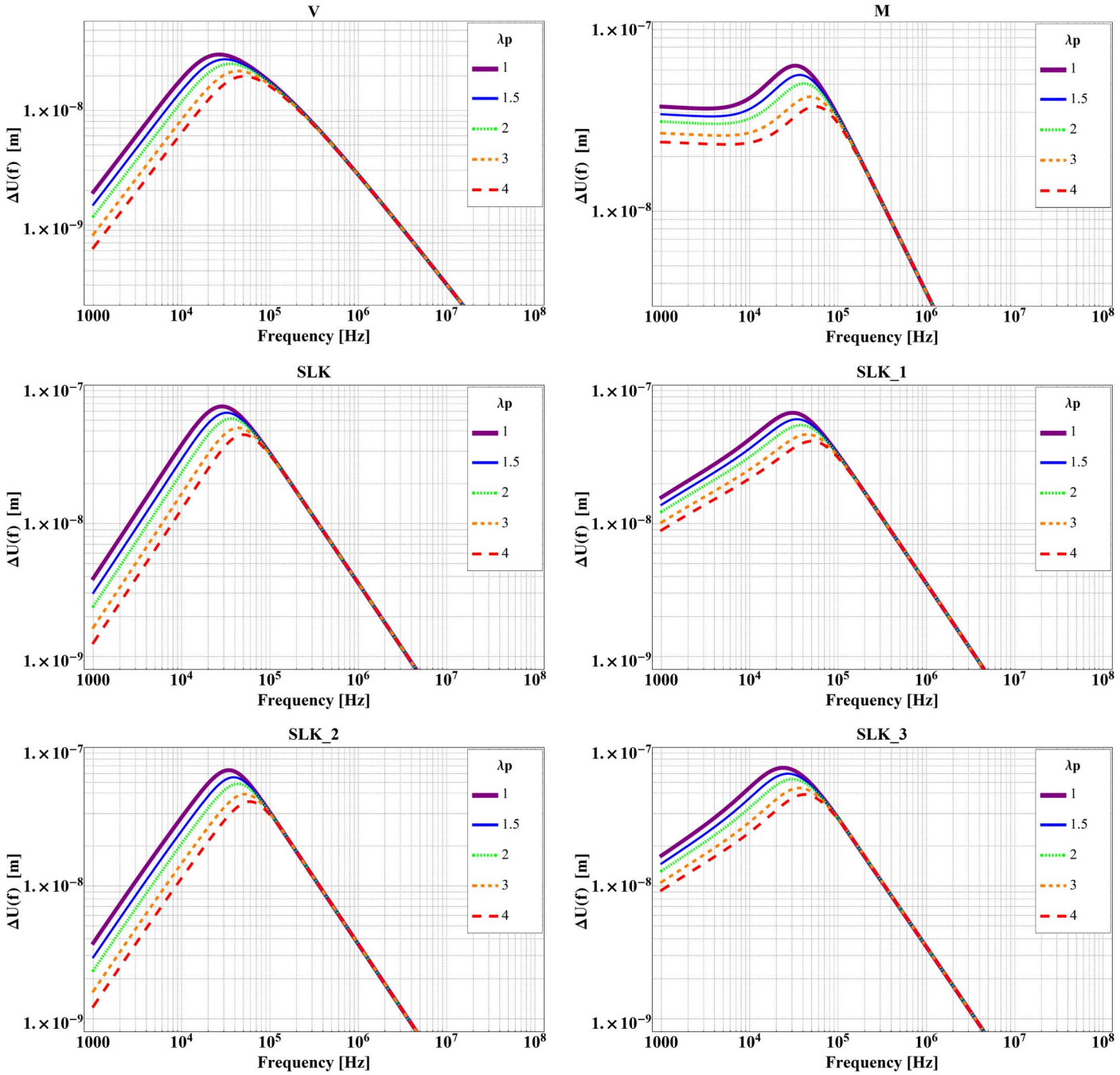

Fig. 7. Sensitivity analysis for the frequency response of the cyclic displacement amplitude of a spherical object ($R = 1$ μm) with respect to its surroundings, with prescribed viscosity ($\mu = 10^{-3}$ Pa · s), tangent Young's modulus ($E = 2.6 \times 109$ Pa), and Poisson's ratio ($\nu = 0.4$) of the microfilaments for a fixed number of active filaments ($n = 50$), varying the level of prestretch ($\lambda_p = 1$, 1.5, 2, 3, and 4); V = Voigt; M = Maxwell; and SLK_1, SLK_2, and SLK_3 = generalized SLK with spring pot in Positions 1, 2, and 3, respectively; $\alpha = 0.5$

that the maximum vibrations $|\Delta U|$ and associated peak frequencies always fall within the interval 10^4 to 10^6 Hz, a range coherent with that experimentally established by several works (e.g., Lejbkowicz and Salzberg 1997; Johns 2002) that still authorize, at least in principle, to think of obtaining resonancelike responses by stimulating single cells by using ultrasounds. Importantly, for all the viscoelastic schemes, the obtained results confirm that US-induced mechanical vibrations, $|\Delta U|$, are mostly comparable (or greater than) spontaneous thermal fluctuations if both calculated in limit situations of pure elastic media, in which the mean square displacement (MSD) is $\langle u_{T,e}^2 \rangle = k_B T / \pi R G$ (Ohshima and Nishio 2001), and pure viscous systems, in which the mean relaxation distance (MRD) is $\langle u_{T,\eta} \rangle = 2R^2 \rho_{ob} v_0 / 9\mu$ (Kittel and Krocmer 1980), with k_B = Botzmann constant; T = absolute temperature; and v_0 = initial velocity. In fact, it can be numerically verified that the MSD maximum square root is of the order of 10^{-9} m, whereas the MRD can oscillate between 10^{-15} and 10^{-8}, in both the cases leading to values smaller than (or at most comparable with) the vibration amplitude peaks obtained theoretically from the aforementioned parametric analyses (Figs. 6–8).

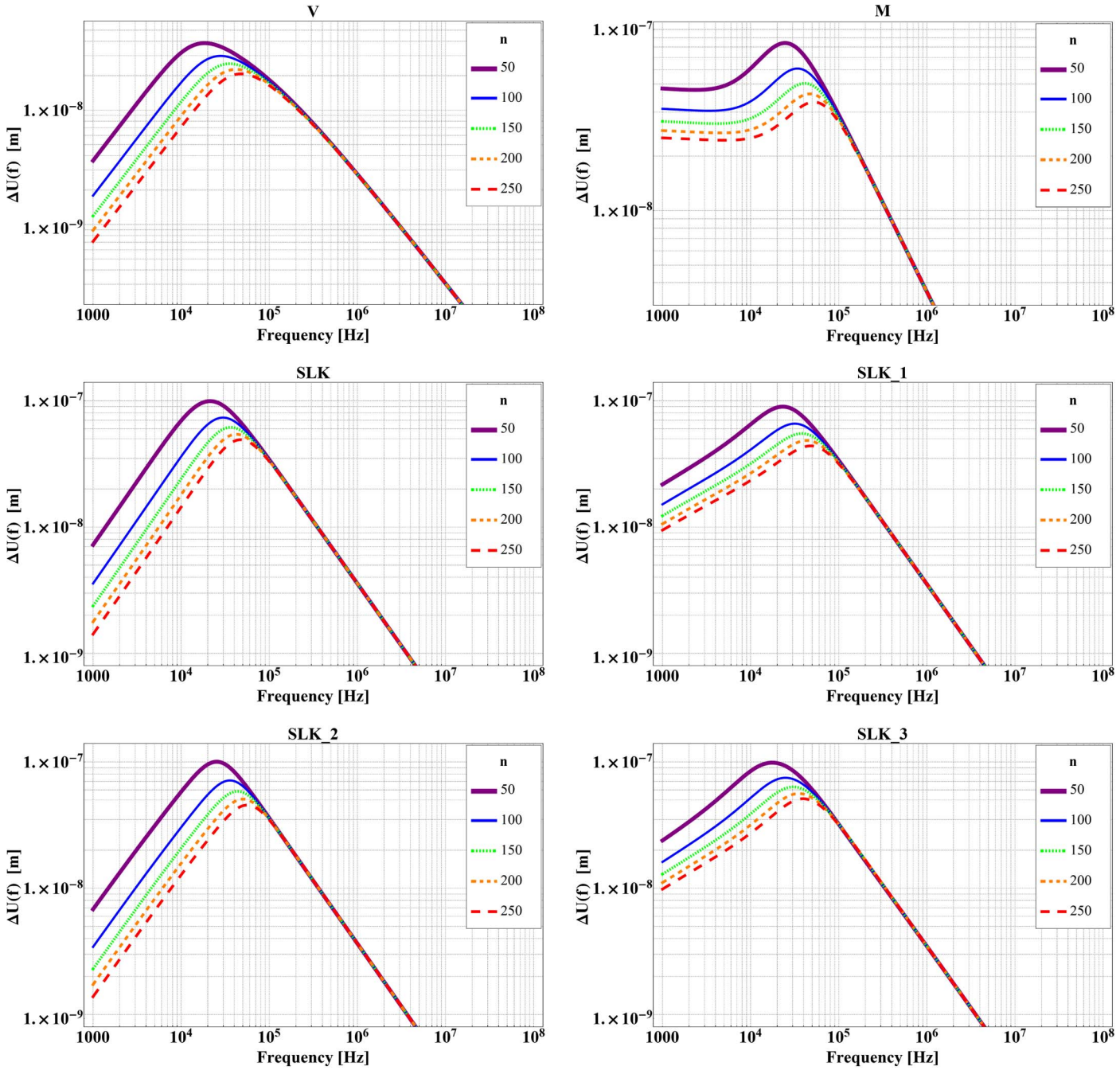

Fig. 8. Sensitivity analysis for the frequency response of the cyclic displacement amplitude of a spherical object ($R = 1$ μm) with respect to its surroundings with prescribed viscosity ($\mu = 10^{-3}$ Pa · s), tangent Young's modulus ($E = 2.6 \times 109$ Pa), and Poisson's ratio ($\nu = 0.4$) of the microfilaments and a fixed level of prestretch ($\lambda_p = 1.3$), varying the number of active microfilaments ($n = 50$, 100, 150, 200, and 250); V = Voigt; M = Maxwell; and SLK_1, SLK_2, and SLK_3 = generalized SLK with spring pot in Positions 1, 2, and 3, respectively; $\alpha = 0.5$

Conclusions and Future Challenges

By following a very recent work by some of the authors aimed to analyze the in-frequency response of single-cell systems to mechanical stimuli (Fraldi et al. 2015), a new enhanced fractional derivative–based viscoelastic scheme incorporating the nonlinear elastic behavior of the cell cytoskeleton has been proposed in this paper by first introducing an elemental subcellular structural model and then following—after a bottom-up procedure to meet the microscale—a small-on-large approach to study the dynamics (nucleus vibration) of the cell as a whole. In this way, along with the geometrical and physical parameters usually involved in the mechanical study of suspended (round) cells, some further key factors influencing the overall stiffness of adherent cells have been taken into account, that is, the prestress/prestretch and the average number of attending protein filaments. Actually, the cell stiffness can significantly change if, by interacting with the ECM, the focal adhesion points invite cell cytoskeleton to assume deformed configurations. Stretching and collective reconfigurations of protein filaments guided by polymerization/depolymerization processes generally accompany the transition of a cell from a suspended to an adherent state. Forces and strains in the prestretched stress fibers

thus play a crucial role in the dynamic updating of the mechanical properties of single cells and in determing their viscoelastic response to mechanical stimuli. In this framework, it has been indeed experimentally shown that low-frequency cyclic loads and strain regimes from 10^{-2} to 10^{-1} can actually generate structural alterations or physical rupture of cytoskeletal elements in living cells (Or and Kimmel 2009). Similar effects have been also observed at relatively high frequencies, particularly for the case of cells stimulated by ultrasound, as found in Mizrahi et al. (2012) and Lejbkowicz and Salzberg (1997), which have shown that configurational and mechanical changes were caused at ultrasonic frequencies (10^6 Hz) by very small strains (10^{-5}) and at physiological frequencies (10^0 Hz) by relatively large strains (10^{-1}).

With reference to the obtained theoretical findings, a rough value of the axial elongation equivalent to a simple uniaxial strain can be roughly estimated as $\varepsilon \propto |\Delta U|/(10 \times R)$: therefore, by recalling that a typical size of a cell nucleus can be found in the interval 2×10^{-7} to 10^{-5} m, whereas vibration magnitudes are obtained from approximately 10^{-9} to 10^{-7} m, strains from 10^{-5} to 10^{-1} can be determined, and higher values can be hence reached because of the prestretch imprisoned in the cytoskeleton filaments of adherent cells.

Also, the peak frequencies, derived from the theory by using the parametric fractional calculus–based viscoelastic schemes, span from tens of kilohertz to approximately 1 MHz, these limit values being both experimentally recognized as critical frequencies at which cells exhibit significant biological configurational alterations attributed to mechanical effects that prevail on thermal ones (Johns 2002; Schuster et al. 2013).

At least in principle, after a few seconds of exposure to ultrasound (e.g., LITUS), cell structural modifications or failure caused by cyclic loading and associated fatigue phenomena could be thus actually expected, and this, on the basis of the ascertained fact that cancer cells are found to be always softer than their normal (healthy) counterparts, independently from the cell line, might pave the way for designing new mechanically based tumor markers and strategies to selectively attack cancer cells.

References

Atanackovic, T. M., Pilipovic, S., and Zorica, D. (2007). "A diffusion wave equation with two fractional derivatives of different order." *J. Phys. A: Math. Theor.*, 40(20), 5319–5333.

Bagley, R. L. (1983). "A theoretical basis for the application of fractional calculus to viscoelasticity." *J. Rheol.*, 27(3), 201.

Bao, G., and Suresh, S. (2003). "Cell and molecular mechanics of biological materials." *Nat. Mater.*, 2(11), 715–725.

Basset, A. B. (1888). *A treatise on hydrodynamics, with numerous examples*, Univ. of Michigan Library, Ann Arbor, MI.

Blair, G. S., and Caffyn, J. (2010). "An application of the theory of quasi-properties to the treatment of anomalous strain-stress relations." *Philos. Mag.*, 40(300), 80–94.

Brennen, C. (1982). "A review of added mass and fluid inertial forces." *Rep. No. CR 82.010*, Dept. of the Navy, Naval Civil Engineering Laboratory, Port Hueneme, CA.

Brunner, C., Niendorf, A., and Käs, J. A. (2009). "Passive and active single-cell biomechanics: A new perspective in cancer diagnosis." *Soft Matter*, 5(11), 2171.

Caille, N., Thoumine, O., Tardy, Y., and Meister, J.-J. (2002). "Contribution of the nucleus to the mechanical properties of endothelial cells." *J. Biomech.*, 35(2), 177–187.

Caputo, M. (1969). *Elasticità e dissipazione*, Zanichelli, Bologna, Italy.

Chen, Q., and Pugno, N. M. (2013). "Bio-mimetic mechanisms of natural hierarchical materials: A review." *J. Mech. Behav. Biomed. Mater.*, 19, 3–33.

Chumakova, O. V., Liopo, A. V., Evers, B. M., and Esenaliev, R. O. (2006). "Effect of 5-fluorouracil, optison and ultrasound on MCF-7 cell viability." *Ultrasound Med. Biol.*, 32(5), 751–758.

Cowin, S. C., and Doty, S. B. (2007). *Tissue mechanics*, Springer, New York.

Cross, S. E., Jin, Y.-S., Rao, J., and Gimzewski, J. K. (2007). "Nanomechanical analysis of cells from cancer patients." *Nat. Nanotechnol.*, 2(12), 780–783.

Cross, S. E., Jin, Y.-S., Tondre, J., Wong, R., Rao, J., and Gimzewski, J. (2008). "AFM-based analysis of human metastatic cancer cells." *Nanotechnology*, 19(38), 384003.

Del Piero, G., and Deseri, L. (1997). "On the concepts of state and free energy in linear viscoelasticity." *Archiv. Rational Mech. Anal.*, 138(1), 1–35.

Delsanto, P. P., Condat, C. A., Pugno, N., Gliozzi, A. S., and Griffa, M. (2008). "A multilevel approach to cancer growth modeling." *J. Theor. Biol.*, 250(1), 16–24.

Deseri, L., Fabrizio, M., and Golden, M. (2006). "The concept of a minimal state in viscoelasticity: New free energies and applications to PDEs." *Archiv. Rational Mech. Anal.*, 181(1), 43–96.

Deseri, L., Paola, M. D., Zingales, M., and Pollaci, P. (2013). "Power-law hereditariness of hierarchical fractal bones." *Int. J. Numer. Methods Biomed. Eng.*, 29(12), 1338–1360.

Deseri, L., Zingales, M., and Pollaci, P. (2014). "The state of fractional hereditary materials (FHM)." *Discrete Continous Dyn. Syst. Ser. B*, 19(7), 2065–2089.

Di Paola, M., Marino, F., and Zingales, M. (2009). "A generalized model of elastic foundation based on long-range interactions: Integral and fractional model." *Int. J. Solids Struct.*, 46(17), 3124–3137.

Di Paola, M., Pinnola, F. P., and Zingales, M. (2013). "A discrete mechanical model of fractional hereditary materials." *Meccanica*, 48(7), 1573–1586.

DuFort, C. C., Paszek, M. J., and Weaver, V. M. (2011). "Balancing forces: Architectural control of mechanotransduction." *Nat. Rev. Mol. Cell Biol.*, 12(5), 308–319.

Ellwart, J. W., Brettel, H., and Kober, L. O. (1988). "Cell membrane damage by ultrasound at different cell concentrations." *Ultrasound Med. Biol.*, 14(1), 43–50.

Faria, E. C., Ma, N., Gazi, E., Gardner, P., Brown, M., Clarke, N. W., and Snook, R. D. (2008). "Measurement of elastic properties of prostate cancer cells using AFM." *Analyst*, 133(11), 1498–1500.

Fraldi, M. (2014). "The mechanichal beauty of hierarchically organized living structures." *Scienza Filosofia*, 11, 13–24.

Fraldi, M., and Cowin, S. C. (2004). "Inhomogeneous elastostatic problem solutions constructed from stress-associated homogeneous solutions." *J. Mech. Phys. Solids*, 52(10), 2207–2233.

Fraldi, M., Cugno, A., Deseri, L., Dayal, K., and Pugno, N. M. (2015). "A frequency-based hypothesis for mechanically targeting and selectively attacking cancer cells." *J. R. Soc. Interface*, 12(111), 20150656.

Grillo, G., Muratori, M., and Punzo, F. (2015). "On the asymptotic behaviour of solutions to the fractional porous medium equation with variable density." *Discrete Continuous Dyn. Syst.*, 35(12), 5927–5962.

Guiot, C., Pugno, N., and Delsanto, P. P. (2006). "Elastomechanical model of tumor invasion." *Appl. Phys. Lett.*, 89(23), 233901.

Haase, K., and Pelling, A. E. (2015). "Investigating cell mechanics with atomic force microscopy." *J. R. Soc. Interface*, 12(104), 20140970–20140970.

Holzapfel, G. A. (2000). *Nonlinear solid mechanics: A continuum approach for engineering*, Wiley, Chichester, U.K.

Honda, H., Kondo, T., Zhao, Q.-L., Feril, L. B., and Kitagawa, H. (2004). "Role of intracellular calcium ions and reactive oxygen species in apoptosis induced by ultrasound." *Ultrasound Med. Biol.*, 30(5), 683–692.

Huang, S., Chen, Z., Pugno, N., Chen, Q., and Wang, W. (2014). "A novel model for porous scaffold to match the mechanical anisotropy and the hierarchical structure of bone." *Mater. Lett.*, 122, 315–319.

Ilinskii, Y. A., Meegan, G. D., Zabolotskaya, E. A., and Emelianov, S. Y. (2005). "Gas bubble and solid sphere motion in elastic media in response to acoustic radiation force." *J. Acoust. Soc. Am.*, 117(4), 2338–2346.

Johns, L. D. (2002). "Nonthermal effects of therapeutic ultrasound: The frequency resonance hypothesis." *J. Athletic Train.*, 37(3), 293–299.
Jonieztz, E. (2012). "Mechanics: The forces of cancer." *Nature*, 491(7425), S56–S57.
Ketene, A. N., Schmelz, E. M., Roberts, P. C., and Agah, M. (2012). "The effects of cancer progression on the viscoelasticity of ovarian cell cytoskeleton structures." *Nanomedicine: Nanotechnol. Biol. Med.*, 8(1), 93–102.
Kittel, C., and Krocmer, H. (1980). *Thermal physics*, W. H. Freeman, San Francisco.
Koeller, R. C. (1984). "Applications of fractional calculus to the theory of viscoelasticity." *J. Appl. Mech.*, 51(2), 299.
Landau, L. D., and Lifshitz, E. M. (1987). "Fluid mechanics." *Course of theoretical physics*, Vol. 6, 2nd Ed., Pergamon, Oxford, U.K.
Lejbkowicz, F., and Salzberg, S. (1997). "Distinct sensitivity of normal and malignant cells to ultrasound in vitro." *Environ. Health Perspect.*, 105(Suppl 6), 1575–1578.
Lejbkowicz, F., Zwiran, M., and Salzberg, S. (1993). "The response of normal and malignant cells to ultrasound in vitro." *Ultrasound Med. Biol.*, 19(1), 75–82.
Lekka, M., et al. (2012a). "Cancer cell detection in tissue sections using AFM." *Archiv. Biochem. Biophys.*, 518(2), 151–156.
Lekka, M., et al. (2012b). "Cancer cell recognition—Mechanical phenotype." *Micron*, 43(12), 1259–1266.
Lekka, M., Laidler, P., Gil, D., Lekki, J., Stachura, Z., and Hrynkiewicz, A. Z. (1999). "Elasticity of normal and cancerous human bladder cells studied by scanning force microscopy." *Eur. Biophys. J.*, 28(4), 312–316.
Li, Q. S., Lee, G. Y. H., Ong, C. N., and Lim, C. T. (2008). "AFM indentation study of breast cancer cells." *Biochem. Biophys. Res. Commun.*, 374(4), 609–613.
Lide, D. R., et al. (2008). *CRC handbook of chemistry and physics*, CRC, Boca Raton, FL.
Mainardi, F. (2012). "An historical perspective on fractional calculus in linear viscoelasticity." *Fract. Calculus Appl. Anal.*, 15(4), 712–717.
Maxey, M. R., and Riley, J. J. (1983). "Equation of motion for a small rigid sphere in a nonuniform flow." *Phys. Fluids*, 26(4), 883.
Metzler, R., and Klafter, J. (2000). "The random walk's guide to anomalous diffusion: A fractional dynamics approach." *Phys. Rep.*, 339(1), 1–77.
Michelet-Habchi, C., et al. (2005). "3D imaging of microscopic structures using a proton beam." *IEEE Trans. Nucl. Sci.*, 52(3), 612–617.
Mizrahi, N., et al. (2012). "Low intensity ultrasound perturbs cytoskeleton dynamics." *Soft Matter*, 8(8), 2438.
Nikkhah, M., Strobl, J. S., De Vita, R., and Agah, M. (2010). "The cytoskeletal organization of breast carcinoma and fibroblast cells inside three dimensional (3-D) isotropic silicon microstructures." *Biomaterials*, 31(16), 4552–4561.
Nutting, P. (1921). "A new general law of deformation." *J. Franklin Inst.*, 191(5), 679–685.
Ohshima, Y. N., and Nishio, I. (2001). "Colloidal crystal: Bead-spring lattice immersed in viscous media." *J. Chem. Phys.*, 114(19), 8649–8658.
Or, M., and Kimmel, E. (2009). "Modeling linear vibration of cell nucleus in low intensity ultrasound field." *Ultrasound Med. Biol.*, 35(6), 1015–1025.
Paszek, M. J., et al. (2014). "The cancer glycocalyx mechanically primes integrin-mediated growth and survival." *Nature*, 511(7509), 319–325.
Podlubny, I. (1999). *Fractional differential equations*. Academic Press, San Diego.
Prabhune, M., Belge, G., Dotzauer, A., Bullerdiek, J., and Radmacher, M. (2012). "Comparison of mechanical properties of normal and malignant thyroid cells." *Micron*, 43(12), 1267–1272.
Pugno, N. M., Bosia, F., and Abdalrahman, T. (2012). "Hierarchical fiber bundle model to investigate the complex architectures of biological materials." *Phys. Rev. E*, 85(1), 011903.
Rebelo, L. M., de Sousa, J. S., Mendes Filho, J., and Radmacher, M. (2013). "Comparison of the viscoelastic properties of cells from different kidney cancer phenotypes measured with atomic force microscopy." *Nanotechnology*, 24(5), 055102.
Rodriguez, M. L., McGarry, P. J., and Sniadecki, N. J. (2013). "Review on cell mechanics: Experimental and modeling approaches." *Appl. Mech. Rev.*, 65(6), 060801.
Schiessel, H., and Blumen, A. (1993). "Hierarchical analogues to fractional relaxation equations." *J. Phys. A: Math. General*, 26(19), 5057–5069.
Schuster, A., et al. (2013). "Cell specific ultrasound effects are dose and frequency dependent." *Ann. Anatomy*, 195(1), 57–67.
Tschoegl, N. (1989). *The phenomenological theory of linear viscoelastic behavior: An introduction*, Springer, New York.
Wolfram, S. (2003). *The mathematica book*, 5th Ed., Wolfram Media, Champaign, IL.